

Non-equilibrium plasma modeling of Gas Tungsten Arc in middle current range

S. Tashiro, T. Iwao*, T. Inaba** and M. Tanaka

Joining and Welding Research Institute, Osaka University, 11-1 Mihogaoka, Ibaraki, Osaka 576-0047

e-mail: tashiro@jwri.osaka-u.ac.jp

*Musashi Institute of Technology, 1-28-1, Tamadutsumi, Setagaya, Tokyo, 158-8577

**Chuo university, 1-13-27 Kasuga, Bunkyo-ku, Tokyo 112-8551

Gas Tungsten Arc (GTA) is suitable as a heat source device for many applications because it can stabilize high temperature arc plasma easily by employing shielding gas. In many cases, MHD simulation model assuming the local thermodynamic equilibrium (LTE) is utilized for analyzing property of GTA. Although the LTE assumption is effective to evaluate high temperature region in the arc column, it is difficult to apply it to low temperature region such as the fringe of the arc column or the sheath regions closed to the electrodes due to decrease of energy exchange. In order to consider the effect of chemical reaction between the arc plasma and the material surface, we have developed a simulation model of GTA assuming chemical and thermal non-equilibrium. In this paper, as a first step of the study, heat source property of argon GTA employing a water-cooled copper anode was simulated.

Key words: Non-equilibrium, Numerical Simulation, Gas Tungsten Arc

1. INTRODUCTION

Gas Tungsten Arc (GTA) is suitable as a heat source device for many applications because it can stabilize high temperature arc plasma easily by employing shielding gas. The arc plasma is produced between a tungsten cathode and an anode material. GTA has many advantages as a heat source device such as high heating efficiency, highly controllable characteristics and low cost for equipment investment. Therefore, it is widely utilized, for example, for production of nano-particles, material processing such as melting, cutting and welding [1], or decomposition, volume reduction and detoxification of toxic waste [2] and so on.

In many cases, MHD simulation model assuming the local thermodynamic equilibrium (LTE) is utilized for analyzing property of GTA because of short calculation time and suitability to couple with other complex processes [3]. Under the LTE assumption, all species in the plasma have the same temperature and its chemical composition is determined depending only on the temperature. This assumption is applicable if the arc plasma has high collision frequency between heavy species (neutral gas and ions) and electrons enough to exchange their thermal energy. Therefore it is considered to be valid only for high temperature plasma with high electron density.

Although the LTE assumption is effective to evaluate high temperature region in the arc column, it is difficult to apply it to low temperature region such as the fringe of the arc column or the sheath regions closed to the electrodes due to decrease of energy exchange. Especially, in order to consider the effect of chemical reaction between the arc plasma and the material surface such as oxidation, non-equilibrium property of the arc plasma should be considered without the LTE assumption, since it is required to understand precise property of the arc plasma closed to the material surface.

A number of numerical modeling of RF plasma

considering non-equilibrium effect has been reported [4, 5]. On the other hand, in case of DC GTA, thermal non-equilibrium model assuming chemical equilibrium was developed [6]. Furthermore, thermal non-equilibrium model including energy balance between the arc and the electrodes was also reported [7]. However, the surface area of the cathode spot was assumed in this model. Although numerical model assuming chemical and thermal non-equilibrium was developed, energy balance between the arc and the electrodes was ignored [8].

Therefore, we have developed a numerical model of GTA assuming chemical and thermal non-equilibrium and including energy balance between the arc and the electrodes. In this paper, as a first step of the study, heat source property of argon GTA employing a water-cooled copper anode was simulated.

2. SIMULATION MODEL

The tungsten cathode, the arc plasma and the water-cooled copper anode are described in a frame of cylindrical coordinate with axial symmetry around the arc axis. The calculation domain is shown in Figure 1. The diameter and the conical angle of the cathode are 3.2mm and 60degrees, respectively. The electrode gap is 5mm. The arc current is 100A. Ar is introduced at the flow rate of 10L/min. from the outside of the cathode on the upper boundary. The flow is assumed to be laminar. The plasma is optically thin. a three component (atoms, ions, electrons), two-temperature argon arc plasma is considered in which atoms and ions have the same translational temperature which is different from that of the electrons. The plasma is assumed to be in chemical (ionization) non-equilibrium and its composition is calculated assuming ionization reactions and diffusion. The other numerical modeling methods are given in detail in our previous papers [9,10]. MHD equations and supplementary equations (1)-(9) are solved iteratively by

the SIMPLER numerical procedure [11].

On the boundaries A-F, C-D and D-F, the temperatures is set to be 300K. The electrical potential is 0V on the boundary C-D and the arc current is given inside the cathode on the boundary A-F. The electron density is $10^{10}/\text{m}^3$ on the boundaries A-F and E-F. Since we neglect the transport of the electrons from the arc plasma to the cathode surface through a cathode sheath, thermal conduction between the electrons and the cathode surface is neglected. On the anode surface B-E, the electron temperature and the electron density can be determined by solving one-dimensional equations of the electron energy conservation and the diffusion along the surface, respectively. In addition, gradient of each physical quantity in radial direction is zero on the arc axis A-C because of the axial symmetry.

Mass conservation equation;

$$\nabla \cdot (\rho \vec{u}) = 0 \quad (1)$$

Momentum conservation equation;

$$\nabla \cdot (\rho \vec{u} \vec{u}) = -\nabla p + \vec{j} \times \vec{B} + \nabla \cdot \tau, \quad \tau_{\alpha\beta} = \eta \left(\frac{\partial u_\alpha}{\partial x_\beta} + \frac{\partial u_\beta}{\partial x_\alpha} \right) \quad (2)$$

Electron energy conservation equation;

$$\vec{u} \cdot \nabla \left\{ n_e \left(\frac{5}{2} k_B T_e + \varepsilon_i \right) \right\} = \nabla \cdot (k_e \nabla T_e) - \left\{ \varepsilon_i + \left(\frac{5}{2} + \frac{e \phi}{k_B \sigma} \right) k_B T_e \right\} \dot{n}_e \quad (3)$$

$$+ \left(\frac{5}{2} + \frac{e \phi}{k_B \sigma} \right) \frac{k_B}{e} \vec{j} \cdot \nabla T_e + \vec{j} \cdot \vec{E} - \frac{3m_e}{m_i} n_e (\bar{\nu}_{ei} + \bar{\nu}_{en}) k_B (T_e - T_h) - \dot{R}$$

Heavy species energy conservation equation;

$$\vec{u} \cdot \nabla \left\{ (n_e + n_n) k_B T_h \right\} = \nabla \cdot (k_h \nabla T_h) + \frac{3m_e}{m_i} n_e (\bar{\nu}_{ei} + \bar{\nu}_{en}) k_B (T_e - T_h) \quad (4)$$

Diffusion equation;

$$\vec{u} \cdot \nabla n_e + \nabla \cdot \left\{ \frac{en_e D_{in}}{k_B T_h} \left(\vec{E} - \frac{1}{en_e} \nabla p_i \right) \right\} = \dot{n}_e \quad (5)$$

Current continuity equation;

$$\nabla \cdot \vec{j} = 0 \quad (6)$$

Generalized Ohm's law;

$$\vec{j} = \sigma \left(\vec{E} - \frac{1}{en_e} \nabla p_e \right) + \phi \nabla T_e \quad (7)$$

Electric field;

$$\vec{E} = -\nabla \Phi \quad (8)$$

Maxwell's equation;

$$\nabla \times \vec{B} = \mu_0 \vec{j} \quad (9)$$

where x is position, ρ is mass density, u is velocity, n is number density, T is temperature, p is pressure, j is current density, B is self-induced magnetic field, τ is stress tensor, E is electric field, Φ is electrical potential, \dot{n}_e ionization rate, D_{in} is diffusion coefficient of ions among neutrals, $\bar{\nu}$: average collision frequency, k_B is Boltzmann constant, μ_0 is permeability of vacuum, e is elementary charge, m is mass, k is translational thermal conductivity, η is dynamic viscosity, ϕ is electron thermodiffusion factor, σ is electrical conductivity, ε_i is ionization potential, \dot{R} is radiation loss, subscript: e, i, n and h are electrons, ions, neutrals, and heavy species (ions and neutrals), z and r are axial and radial component, α and β are z or r . the transport coefficients are calculated as function of number density and collision frequency as follows:

$$k_e = a''(T_e) \cdot 3.203 \frac{n_e k^2 T_e}{m_e \nu_{ei}} \quad (10)$$

$$\phi = a'''(T_e) \cdot 1.389 \frac{en_e k}{m_e \nu_{ei}} \quad (11)$$

$$k_h = \frac{15}{8} k \bar{C}_i (n_e \lambda_i + n_n \lambda_n) \quad (12)$$

$$D_{in} = \frac{\bar{C}_i}{\sqrt{2} (n_e + n) \bar{Q}_m} \quad (13)$$

$$\sigma = a'(T_e) \cdot 1.975 \frac{n_e e^2}{m_e \nu_{ei}} \quad (14)$$

where \bar{C} is average thermal speed, \bar{Q} is collision cross section and a', a'' and a''' are factors to express influence of electron-neutral collision. The energy transport due to the ionization reaction is expressed in the second term on the right hand side of Eq. (4). In addition, the energy transport due to the diffusion was ignored as the previous study [10].

In the solution of Eqs. (1)-(9), special account needs to be taken at the electrode surface for effects of energy that only occur at the surface. At the cathode surface, additional energy flux terms need to be considered for radiation cooling, thermionic cooling due to the emission of electrons and ion heating. The additional energy flux for the cathode H_K is:

$$H_K = -\varepsilon \alpha T^4 - |j_e| \phi_{wc} + |j_i| V_i \quad (15)$$

where ε is the surface emissivity, α is the Stefan-Boltzmann constant, ϕ_{wc} is the work function of the tungsten cathode, V_i is the ionization potential of argon, j_e is the electron current density, and j_i is the ion current density. At the cathode surface, for thermionic

emission of electrons, j_e cannot exceed the Richardson current density J_R [12] given by:

$$|J_R| = AT^2 \exp\left(-\frac{e\phi_e}{k_B T}\right) \quad (16)$$

where A is the thermionic emission constant for the cathode surface, ϕ_e is the effective work function for thermionic emission of the electrode surface at the local surface temperature, and k_B is the Boltzmann's constant. The ion-current density j_i is then assumed to be $|j_i| = |j_R|$ if $|j_i|$ is greater than $|j_R|$; where $|j| = |j_e| + |j_i|$ is the total current density at the cathode surface obtained from Eq. (6)

Similarly, for the anode surface, additional energy flux terms need to be considered for radiation cooling, electron enthalpy transport, electron condensation, ion recombination and the additional energy flux for the anode H_A is:

$$H_A = -\varepsilon\alpha T^4 + \left[\left(\frac{5}{2} + \frac{e\phi}{k_B\sigma} \right) \frac{k_B T_e}{e} + \phi_{wa} \right] |j_e| + |j_i| V_i \quad (17)$$

where ϕ_{wa} is the work function of the copper and $|j_i|$ is the current density at the anode surface obtained from Eq. (6).

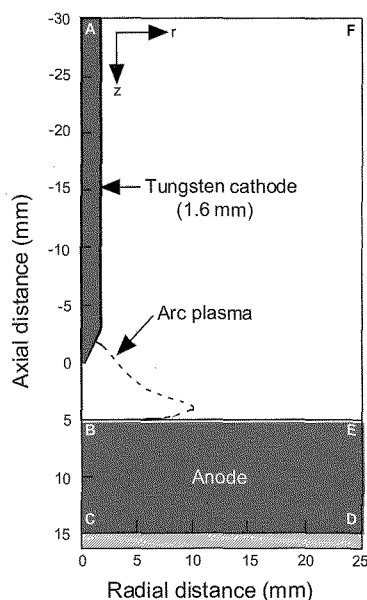


Fig. 1. Schematic illustration of simulation domain.

3. RESULTS AND DISCUSSION

Figure 2 and 3 show two-dimensional temperature distribution of electron and heavy species in addition to the electrodes, respectively. It is seen that the electron temperature agrees with the heavy species temperature near the arc axis and the LTE approximation is valid in this region. Both temperatures near the cathode tip reach 15000K. This result approximately agrees with experimental result [13]. On the other hand, it is obvious that in region closed to both electrodes and outside the

fringe of the arc column the electron temperature exceeds the heavy species temperature and non-equilibrium characteristics appears. The radius of the arc column seen in the electron temperature distribution is obviously larger than that of heavy species. In addition, the max. surface temperatures of the cathode and anode reach 3600K and 700K, respectively.

Figure 4 shows dependence of temperature of electron and heavy species near the anode surface on axial distance from the cathode tip. The axial position of 5mm indicates the anode surface. It was found that non-equilibrium property appears in the region where temperature decreases below 10000K. and this region has thickness of 0.7mm. The temperature difference between electron and heavy species occurs due to decrease of collision frequency.

Figure 5 shows dependence of electron density and collision frequency between electron and heavy species near the anode surface on axial distance from the cathode tip. It can be seen that the electron density and the collision frequency decrease with approach to the anode surface. The electron density becomes 2×10^{22} where the plasma temperature decreases to 10000K. Consequently it was found that non-equilibrium property appears below the collision frequency of 2×10^{11} corresponding to this electron density.

Figure 6 shows dependence of heat intensity onto the anode on radial distance from the arc axis. Each component of heat intensity calculated by equation (17), that due to thermal conduction and total heat intensity which is sum of each component are presented. It was found that the heat intensity due to electron absorption onto the anode (electron condensation and electron enthalpy) is significant compared with that of thermal conduction and that of ion recombination is negligibly small.

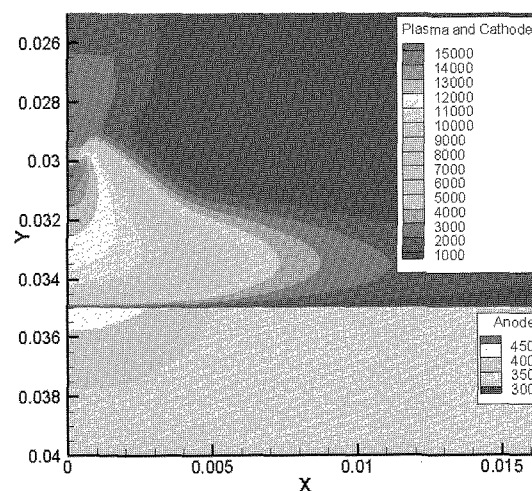


Fig. 2. Two-dimensional temperature distribution of heavy species and electrodes.

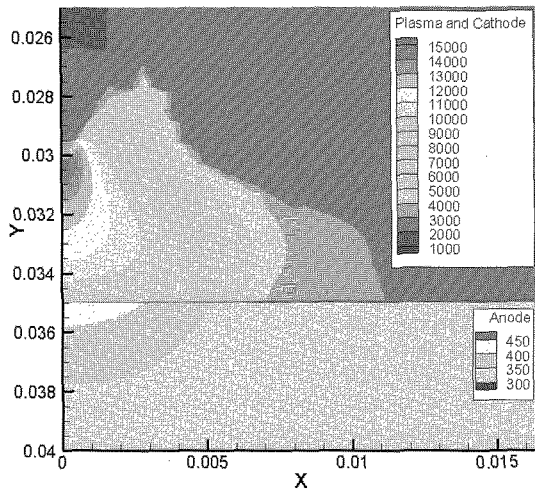


Fig. 3. Two-dimensional temperature distribution of electron and electrodes.

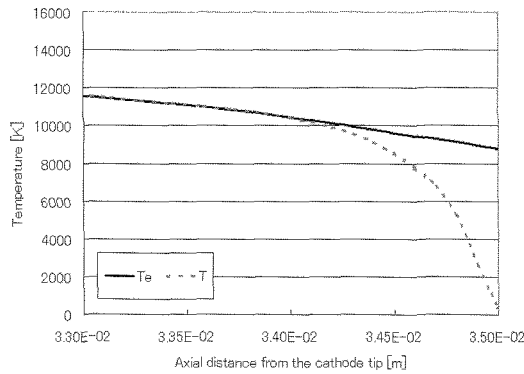


Fig. 4. Dependence of temperature of electron and heavy species on axial distance from the cathode tip..

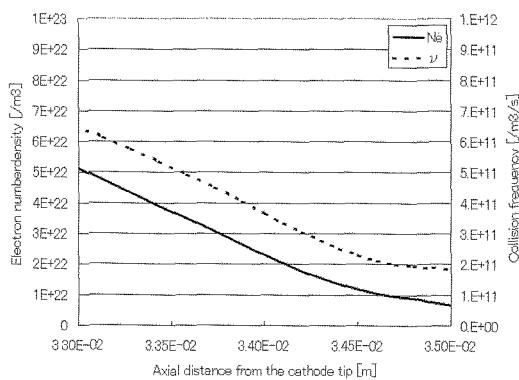


Fig. 5. Dependence electron density and collision frequency on axial distance from the cathode tip.

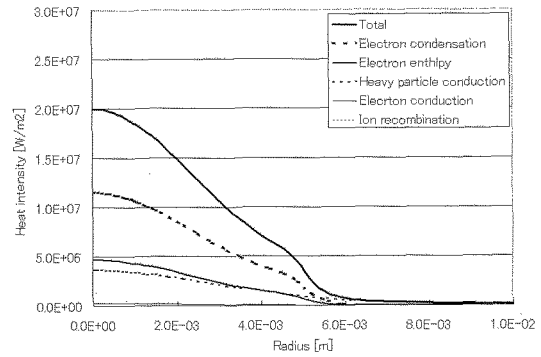


Fig. 6. Dependence of heat intensity onto the anode surface on radial distance from the arc axis

4. CONCLUSIONS

The main conclusions are summarized as follows:

- 1) The simulation result of the max. plasma temperature of 15000K approximately agrees with the experimental result.
- 2) The LTE assumption is valid near the arc axis except for the region near the electrodes.
- 3) The non-equilibrium property appears below the collision frequency of $2 \cdot 10^{11}$ corresponding to the plasma temperature of 10000K. The thickness of this region becomes approximately 0.7mm near the anode surface.
- 4) The heat intensity onto the anode surface due to electron absorption onto the anode (electron condensation and electron enthalpy) is significant compared with that of thermal conduction and that of ion recombination is negligibly small.

References

[1] M. Ushio, et.al., *IEEE Trans. P. S.*, **32**, 108 (2004).
 [2] T. Inaba, et.al, *IEEE Trans. D. E. I*, **7**, 684 (2000).
 [3] M. Tanaka, et.al., *Vacuum*, **73**, 381 (2004).
 [4] Y. Tanaka, *J. Phys. D: Appl. Phys.*, **37**, 1190 (2004).
 [5] T. Watanabe and N. Sugimoto, *Thin Solid Films*, **457**, 201 (2004).
 [6] K. C. Hsu and E. Pfender *J. Appl. Phys*, **54**, 4359 (1983).
 [7] J. Haidar, *J. Phys. D: Appl. Phys.*, **32**, 263 (1999).
 [8] J. Jenista and J. V. R. Heberlein *IEEE Trans. P. S.*, **25**, 883 (1997).
 [9] S. Tashiro, et.al., *ISPC17*, 205 (2005).
 [10] M. Tanaka, et.al., *Plasma Chem. Plasma Process*, **23**, 585-606 (2003).
 [11] S. V. Patanker, "Numerical heat transfer and fluid flow" Washington DC, Hemisphere Publishing Corporation, 1980
 [12] E. Pfender, "Electric Arcs and Arc Gas heaters, Ch. 6", published in M. H. Hirsh and H. J. Oskam, *Gaseous Electronics*, Academic Press, New York (1978) 291-398.
 [13] K. C. Hsu, et.al., *J. Appl. Phys.*, **54**, 1293 (1983)